Energy localization and transport in binary waveguide arrays

Matteo Conforti,[1] Costantino De Angelis,[1,*] and T. R. Akylas[2]
[1]*CNISM, Dipartimento di Ingegneria dell'Informazione, Università degli Studi di Brescia, Brescia 25123, Italy*
[2]*Department of Mechanical Engineering, Massachusetts Institute of Technology, Cambridge, Massachusetts 02139, USA*
(Received 14 December 2010; published 18 April 2011)

We obtain solitary-wave solutions of a model describing light propagation in binary (linearly and nonlinearly) waveguide arrays. This model describes energy localization and transport in various physical settings, ranging from metal-dielectric (i.e., plasmonic) to photonic crystal waveguides. The solitons exist for focusing, defocusing, and even for alternating focusing-defocusing nonlinearity.

DOI: 10.1103/PhysRevA.83.043822 PACS number(s): 42.65.Tg, 73.20.Mf, 78.67.Pt

I. INTRODUCTION

Discrete optics in coupled waveguides has been an area of intense research activities during the last three decades (see [1] for a recent review). Most efforts have been devoted to the analysis of linear and nonlinear properties of uniform waveguide arrays, i.e., arrays composed of equally spaced identical waveguides, and both one-dimensional and multidimensional configurations have been considered theoretically as well as experimentally [2–8].

On the other hand, nonuniform waveguide arrays offer a richer setting where engineering of the periodic structure can provide further degrees of freedom. In this context, zigzag waveguide arrays (i.e., the cascade of arrays characterized by alternating tilt angles) have been introduced to get diffraction management [9]. Binary arrays composed of waveguides with different wave numbers have been thoroughly studied (see [10–13] and related works) since they exhibit interesting features, such as double refraction, due to their intrinsic two-band nature. Moreover, binary arrays with different coupling coefficients have been considered, since they might offer a more feasible experimental framework in which to exploit a two-band structure in the linear and nonlinear regimes [14,15]. In this instance, the use of photonic crystal waveguides [16] or waveguides based on plasmonic confinement [17,18] offers a unique setting in which to exploit propagation in the so-called alternating positive and negative coupling regime [19,20]. Efremidis *et al.* [20], in particular, studied nonlinearly uniform arrays where the coupling coefficients are equal in modulus but of opposite sign. In this case the structure does not possess a gap in the linear spectrum, and can be reduced to a uniform array by a phase transformation. Exploiting this transformation, families of discrete solitons were calculated starting from the well-known discrete Schrödinger equation.

In this paper we consider a binary array designed in such a way that the coupling between successive waveguides switches periodically from C to $-C(1+\epsilon)$, thus opening a gap centered at zero Bloch momentum in the linear dispersion relation. We consider also a binary Kerr nonlinearity and we look for self-sustained nonlinear propagation in the form of gap solitons in such a structure. Specifically, extending previously derived results [21–30], we obtain in the continuum limit exact analytical solutions for both stationary and "walking" gap solitons moving along the spatial coordinate with a tunable velocity.

*costantino.deangelis@ing.unibs.it

II. THEORETICAL MODEL AND SOLITON SOLUTIONS

According to coupled mode theory and taking into account third-order nonlinearities in the form of a pure Kerr effect, the governing equations read as [10]

$$i E'_{nz} + \beta_n E'_n + C_{n-1} E'_{n-1} + C_{n+1} E'_{n+1} + \chi_n |E'_n|^2 E'_n = 0,$$

where E'_n is the amplitude of the modal field $M_n(x)$ of the nth waveguide; β_n is the propagation constant of each individual waveguide ($\beta_n = \beta + \Delta\beta/2$ for n even and $\beta_n = \beta - \Delta\beta/2$ for n odd); χ_n, the site-dependent nonlinear coefficient, is γ_1 (γ_2) for n even (odd); and C_{n-1},C_{n+1} are the coupling coefficients with the $(n-1)$th and the $(n+1)$th waveguides, respectively. In the specific case of interest, $C_{n-1} = C_1$ and $C_{n+1} = C_2$ when n is even, whereas $C_{n-1} = C_2$ and $C_{n+1} = C_1$ when n is odd. We then perform the transformation $E'_n = E_n \exp(i\beta z)$ and we separately consider the mode amplitudes in the even and odd waveguides. Finally, $E_{2n} = A_n$ and $E_{2n-1} = B_n$ are governed by the following two sets of coupled equations with constant coefficients:

$$\begin{aligned} i A_{nz} + \frac{\Delta\beta}{2} A_n + C_1 B_n + B_{n+1} + \gamma_1 |A_n|^2 A_n = 0, \\ i B_{nz} - \frac{\Delta\beta}{2} B_n + A_{n-1} + C_1 A_n + \gamma_2 |B_n|^2 B_n = 0, \end{aligned} \tag{1}$$

where C_2 has been set equal to 1, without loss of generality.

Assuming Bloch-wave disturbances, $(A_n, B_n) \propto \exp\{i(nk_x + k_z z)\}$, the linear dispersion relation of Eqs. (1) reads

$$k_z^2 = \left(\frac{\Delta\beta}{2}\right)^2 + C_1^2 + 1 + 2C_1 \cos k_x.$$

Note that a band gap opens whenever $\Delta\beta \neq 0$ and/or for $C_1 \neq \pm 1$, the band edges corresponding to the wave number $k_x = 0$ for $C_1 < 0$ and $k_x = \pi$ for $C_1 > 0$. Moreover, there is numerical evidence [10,28] that discrete solitons can reside inside this gap. We shall make a comprehensive analytical study of stationary and moving gap solitons on the basis of an equivalent continuous model.

Specifically, for $C_1 < 0$, in the neighborhood of $k_x = 0$, we use the expansions

$$\begin{aligned} A_{n\pm1}(z) &= u(x,z) \pm u_x(x,z) + \tfrac{1}{2} u_{xx}(x,z) + \cdots, \\ B_{n\pm1}(z) &= w(x,z) \pm w_x(x,z) + \tfrac{1}{2} w_{xx}(x,z) + \cdots \end{aligned}$$

to obtain (as a first-order approximation)

$$\begin{aligned} iu_z + \frac{\Delta\beta}{2}u + w_x + \epsilon w + \gamma_1|u|^2u = 0, \\ iw_z - \frac{\Delta\beta}{2}w - u_x + \epsilon u + \gamma_2|w|^2w = 0, \end{aligned} \tag{2}$$

where $C_1 = -1+\epsilon$. This equation system also arises in the neighborhood of $k_x = \pi$ for $C_1 = 1+\epsilon$, following a similar expansion procedure after the change of variables $(A_n, B_n) \to (-1)^n(A_n, B_n)$.

We now look for both stationary and walking self-confined solutions of the system defined by Eqs. (2). To this end, we use the following trial functions [23]:

$$\begin{aligned} u(x,z) &= \tfrac{1}{2}[K_1 g_1(\xi) + iK_2 g_2(\xi)]\exp(i\psi\cos Q), \\ w(x,z) &= \tfrac{1}{2i}[K_1 g_1(\xi) - iK_2 g_2(\xi)]\exp(i\psi\cos Q), \\ \xi &= \frac{x+vz}{\sqrt{1-v^2}}, \quad \psi = \frac{vx+z}{\sqrt{1-v^2}}, \\ K_1 &= \left(\frac{1+v}{1-v}\right)^{1/4}, \quad K_2 = \left(\frac{1-v}{1+v}\right)^{1/4} \end{aligned} \tag{3}$$

with $g_{1,2}$ two arbitrary complex functions, $-1 \leqslant v \leqslant 1$ and $0 \leqslant Q \leqslant \pi$. Although not necessary, for the sake of simplicity, from now on we set $\Delta\beta = 0$ (i.e., the biatomic nature of the array is left to the coupling coefficients only).

Substitution of the ansatz (3) into Eqs. (2) gives ($s = \gamma_1 + \gamma_2$, $d = \gamma_1 - \gamma_2$)

$$\begin{aligned} &-\dot{g}_1 + i\cos(Q)g_1 + i\epsilon g_2 + \frac{s}{8i}\left(K_1^4|g_1|^2g_1 + 2|g_2|^2g_1 - g_2^2g_1^*\right) \\ &\quad -\frac{d}{8}\left(-K_2^2|g_2|^2g_2 - 2K_1^2|g_1|^2g_2 + K_1^2g_1^2g_2^*\right) = 0, \\ &\dot{g}_2 + i\cos(Q)g_2 + i\epsilon g_1 + \frac{s}{8i}\left(K_2^4|g_2|^2g_2 + 2|g_1|^2g_2 - g_1^2g_2^*\right) \\ &\quad -\frac{d}{8}\left(K_1^2|g_1|^2g_1 + 2K_2^2|g_2|^2g_1 - K_2^2g_2^2g_1^*\right) = 0. \end{aligned}$$

These equations have the invariant $P = |g_1|^2 - |g_2|^2$; as we are interested in bright solitons, we set $P = 0$, so that $|g_1|^2 = |g_2|^2$ and $g_{1,2}(\xi) = f(\xi)\exp[i\theta_{1,2}(\xi)]$. Finally, using $\eta = f^2$ and $\mu = \theta_1 - \theta_2$, we get

$$\begin{aligned} \dot{\eta} &= -\frac{\partial H}{\partial \mu}, \quad \dot{\mu} = \frac{\partial H}{\partial \eta}, \\ H &= 2\eta(\epsilon\cos\mu + \cos Q) \\ &\quad -\frac{s}{8}\eta^2\left(\frac{K_1^4}{2} + \frac{K_2^4}{2} + 2 - \cos(2\mu)\right) \\ &\quad -\frac{d}{4}\eta^2\left(K_1^2 + K_2^2\right)\sin\mu. \end{aligned} \tag{4}$$

Equations (4) represent a one-dimensional (thus integrable) Hamiltonian system, and solitary-wave solutions correspond to the separatrix trajectories that are homoclinic to (i.e., emanate from and return to) the unstable fixed points of (4). In the following we assume $s > 0$, since the results can be easily extended to the case $s < 0$ by the substitution $\mu \to \mu + \pi$, $Q \to \pi - Q$.

Bright solitons emanate from the unstable fixed point $(\eta_0, \mu_0) = (0, \pm\arccos[-\cos(Q)/\epsilon])$ and correspond to level curves of the Hamiltonian $H(\eta_0, \mu_0) = 0$. By exploiting $H = 0$, we can derive the expression of η as a function of μ from the definition of H:

$$\eta = \frac{16(\epsilon\cos\mu + \cos Q)}{s\left[\frac{K_1^4}{2} + \frac{K_2^4}{2} + 2 - \cos(2\mu)\right] + 2d\left(K_1^2 + K_2^2\right)\sin\mu}. \tag{5}$$

By inserting Eq. (5) into $\dot{\mu} = \frac{\partial H}{\partial \eta}$, it follows that

$$\dot{\mu} = -2(\cos Q + \epsilon\cos\mu). \tag{6}$$

This equation can be easily integrated to obtain

$$\mu(\xi) = -2\arctan\left[\sqrt{\frac{\epsilon+\cos Q}{\epsilon-\cos Q}}\tanh[\sqrt{\epsilon^2 - \cos(Q)^2}\,\xi]\right]. \tag{7}$$

and, upon substitution in Eq. (5),

$$\eta(\xi) = \frac{\operatorname{sech}(\delta\xi)^2(\cos Q + \epsilon)}{-4db_1\alpha\tanh(\delta\xi) + sb_2[1 + \alpha^2\tanh(\delta\xi)^2] - 2s\frac{[1-\alpha^2\tanh(\delta\xi)^2]^2}{1+\alpha^2\tanh(\delta\xi)^2}}, \tag{8}$$

where $\alpha = \sqrt{\frac{\epsilon+\cos(Q)}{\epsilon-\cos(Q)}}$, $\delta = \sqrt{\epsilon^2 - \cos(Q)^2}$, $b_1 = K_1^2 + K_2^2$, $b_2 = \frac{K_1^4}{2} + \frac{K_2^4}{2} + 3$.

Once we get the solutions $\eta(\xi)$ and $\mu(\xi)$, we can find the fields $u(x,z)$ and $w(x,z)$ by substitution in (3) and solving

$$\begin{aligned} \dot{\theta}_1 &= \cos Q + \epsilon\cos\mu - \frac{s}{8}\eta\left[K_1^4 + 2 - \cos(2\mu)\right] \\ &\quad -\frac{d}{8}\eta\left(3K_1^2 + K_2^2\right)\sin\mu. \end{aligned} \tag{9}$$

The expression of θ_1 is rather cumbersome except for stationary solutions ($v = 0$). In fact by inserting (5) and (6) in (9) it is straightforward to show that $\theta_1 = \mu/2$.

We now focus our attention on the existence domain for bright gap solitons. These solitons belong to a family with two free parameters: the velocity v ($-1 \leqslant v \leqslant 1$) and Q ($\arccos\epsilon \leqslant Q \leqslant \pi - \arccos\epsilon$). From Eq. (5) we note, however, that, as the array parameters (ϵ,s,d) are changed, the amplitude η can diverge at some points, entailing that some (v, Q) couples are not allowed.

More specifically, for a given Q, we find that $\eta(\xi)$ is bounded for all ξ, and bright soliton solutions can exist only above a critical velocity v; as long as $s > |d|$ this critical velocity is 0 so that all possible v and Q values in the (Q,v) plane can be attained; however, when $|d| \geqslant s$ a different situation arises: for $\arccos\epsilon \leqslant Q \leqslant \pi/2$, solutions only exist above a critical velocity v_{cr}:

$$|v_{cr}| = \frac{\sqrt{2}}{s}\sqrt{s^2 - d^2 + |d|\sqrt{d^2 - s^2}}. \tag{10}$$

For $\pi/2 \leqslant Q \leqslant \pi - \arccos\epsilon$ such a critical velocity does not exist; however, bright soliton solutions are permitted only for $Q \geqslant \pi - \arccos(\epsilon\sqrt{t})$ with t given by

$$t = \frac{s^2(3+f_1) - (df_2)^2 + \sqrt{(df_2)^4 - 2s^2d^2f_2^2(1+f_1)}}{2s^2}, \tag{11}$$
$$f_1 = \frac{K_1^4 + K_2^4}{2}, \quad f_2 = K_1^2 + K_2^2.$$

This last condition can be derived by looking at the phase plane (η,μ). When $Q = \pi - \arccos(\epsilon\sqrt{t})$, another unstable fixed point exists characterized by $\mu_p = -\mathrm{sgn}(d)\arccos[-\cos(Q)/\epsilon)]$, $\eta_p = 8\epsilon^2\sqrt{1-\cos(Q)^2/\epsilon^2}\sec(Q)/[-|d|(K_1^2+K_2^2) + 2s\sqrt{1-\cos(Q)^2/\epsilon^2}]$ and having Hamiltonian $H(\eta_p,\mu_p) = 0$. In this instance the separatrix trajectory is heteroclinic, connecting the points (η_0,μ_0) and (η_p,μ_p), and the resulting solution corresponds to a kink soliton. If we increase Q above this threshold, the trajectories in the phase plane become unbounded, preventing the existence of localized solutions.

The existence conditions on v and Q can be easily translated into conditions on the soliton transverse phase $k_x = v\cos(Q)/(\sqrt{1-v^2})$ and propagation constant $k_z = \cos(Q)/(\sqrt{1-v^2})$, as illustrated in Fig. 1.

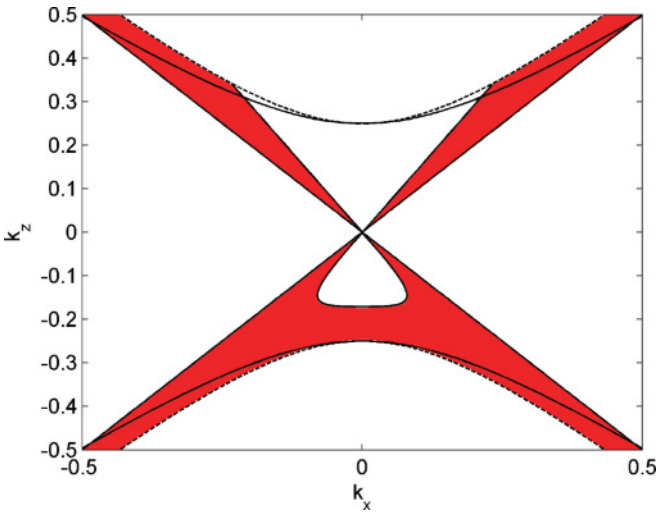

FIG. 1. (Color online) Existence conditions on k_x and k_z. Continuous line refers to the dispersion relation of the discrete problem; dashed line shows the dispersion relation of the continuous approximation and the filled region corresponds to the existence domain of the gap soliton solutions ($\epsilon = 0.25$, $s = 2$, $d = 2.1$).

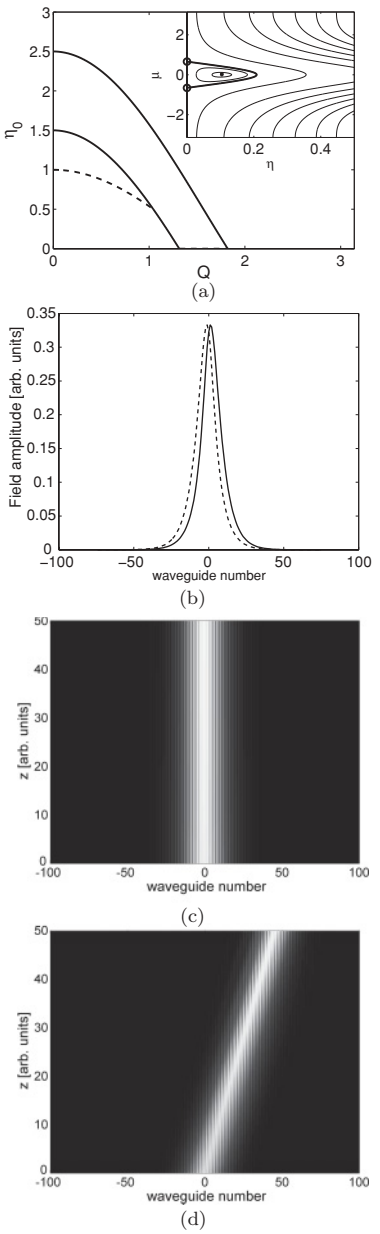

FIG. 2. (a) Bifurcation diagram of the Hamiltonian system ($v = 0$): continuous line for stable centers, dashed line for unstable saddles; inset shows phase plane for $Q = 1.77$ (open circle indicates saddle, filled circle indicates stable center); (b) field amplitude in even (continuous) and odd (dashed) waveguides ($v = 0$); (c) field evolution along the array for $v = 0$; (d) field evolution along the array for $v = 0.5$. In all panels, $\epsilon = 0.25$, $Q = 1.77$, $s = 2$, $d = 0$.

III. EXAMPLES

In this section, we discuss some specific examples of the soliton solutions derived earlier. We also show the robustness of our solutions in some representative cases where we consider propagation in different arrays.

As a first example, we consider an array with all the waveguides having the same nonlinear response ($s = 2, d = 0$). In this case, bright soliton solutions do exist for $\arccos\epsilon \leqslant Q \leqslant \pi - \arccos\epsilon$ as one can also infer from the bifurcation diagram of Fig. 2(a), that shows the amplitude η_0 of the

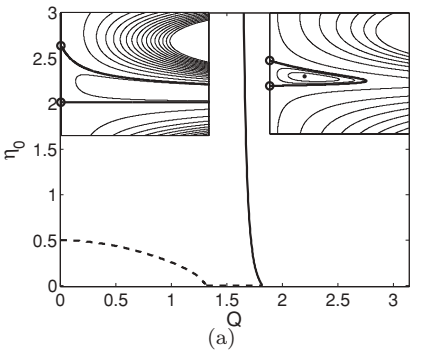

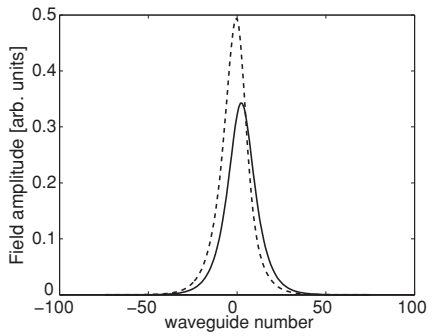

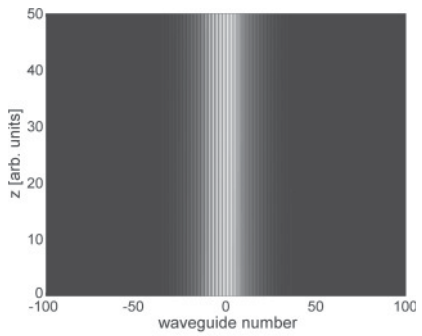

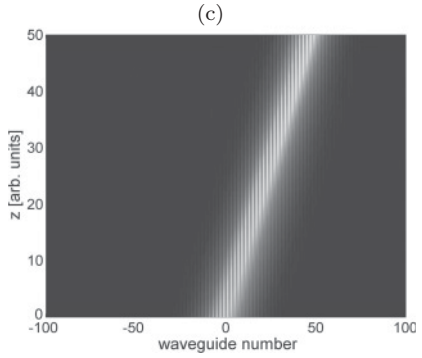

FIG. 3. (a) Bifurcation diagram of the Hamiltonian system ($v = 0$): continuous line for stable centers, dashed line for unstable saddles; left (right) inset shows phase plane for $Q = 1.5$ ($Q = 1.77$) (open circle indicates saddle, filled circle indicates stable center); (b) field amplitude in even (continuous) and odd(dashed) waveguides ($v = 0$); (c) field evolution along the array for $v = 0$; (d) field evolution along the array for $v = 0.5$. In all panels, $\epsilon = 0.25$, $Q = 1.77$, $s = 2$, $d = 2$.

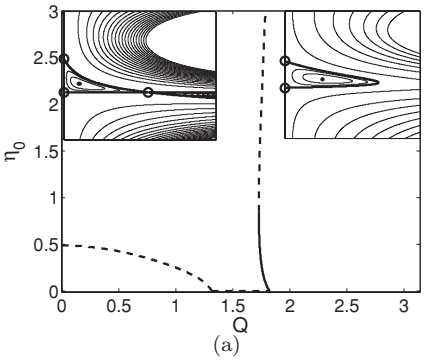

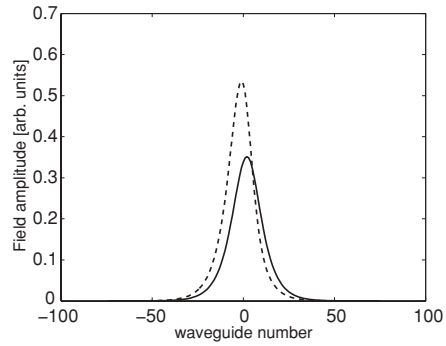

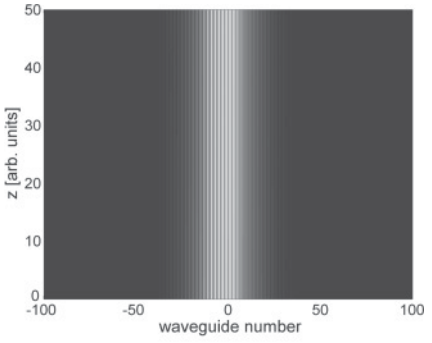

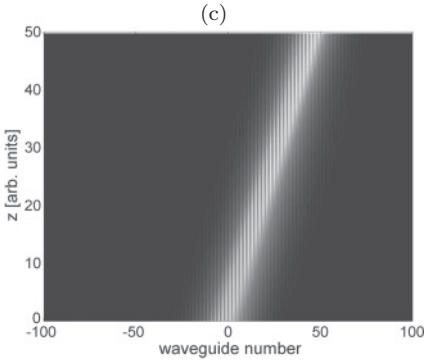

FIG. 4. (a) Bifurcation diagram of the Hamiltonian system ($v = 0$): continuous line for stable centers, dashed line for unstable saddles; left (right) inset shows phase plane for kink (bright) soliton (open circle indicates saddle, filled circle indicates stable center); (b) field amplitude in even (continuous) and odd (dashed) waveguides ($v = 0$); (c) field evolution along the array for $v = 0$; (d) field evolution along the array for $v = 0.5$. In all panels, $\epsilon = 0.25$, $Q = 1.77$, $s = 2$, $d = 2.1$.

fixed points of system (4) as a function of the parameter Q. In fact, in this interval both the unstable saddle $\eta_0 = 0$ and a stable center with $\eta_0 \neq 0$ exist. From the phase plane depicted in the inset (corresponding to $Q = 1.77$), it is evident that the separatix describing the soliton emanates from $(\eta_0, \mu_0) = (0, \arccos[-\cos(Q)/\epsilon])$, turns around the center and returns to the fixed point with vanishing η. Note that in this situation ($d = 0$) the $v = 0$ case shows perfect mirror symmetry between the field in the even and odd sites [see Fig. 2(b)]; as d increases this mirror symmetry is obviously lost. Figures 2(c) and 2(d) show the propagation of a stationary ($v = 0$) and a moving ($v = 0.5$) soliton.

The second example we are considering in this section corresponds to $s = 2, d = 2$ (i.e., an interlaced linear-nonlinear array). As one can see from Fig. 3(a), for this choice of parameters bright soliton solutions for $v = 0$ exist only for $\pi/2 < Q \leqslant \pi - \arccos\epsilon$, because the stable center does not exist for $Q < \pi/2$. In this instance, the phase portrait is qualitatively different for Q greater or less than $\pi/2$ [right and left insets of Fig. 3(a)]. For $Q > \pi/2$ the phase portrait is similar to the $d = 0$ case, except for the asymmetry with respect to μ. For $Q < \pi/2$ the separatrix emanating from the saddle is not closed and separates orbits of unbounded motion from periodic motion. As a consequence solitons do not exist.

It is remarkable to note that even in the case of interlaced focusing-defocusing nonlinearities soliton solutions still exist as clearly demonstrated in Fig. 4 for $s = 2, d = 2.1$; this applies also to solutions walking along the array as shown in Fig. 4(d). Note also that, as can be seen from Fig. 4(a), in this case we do not have bright soliton solutions for $Q < 1.73$; however, as we have already noted above, in the presence of a nonzero transverse velocity we have access to this region of Q values. This is what we can see in Fig. 5 where propagation in an interlaced focusing-defocusing array is shown for $Q = 1.72$ and $v = 0.5$; note that, remarkably, this last case corresponds to a situation where we do not have bright soliton solutions with zero transverse velocity.

Another interesting feature of the interlaced focusing-defocusing case is the existence of flat-top and kink solitons, due to the presence of an additional saddle in the bifurcation diagram. It is possible that the two saddles possess the same

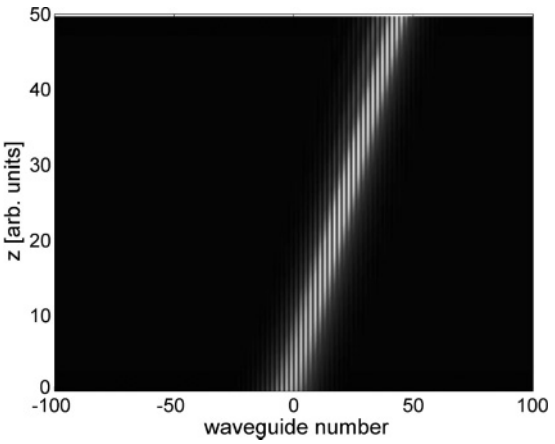

FIG. 5. Field evolution along the array for $v = 0.5$; here $\epsilon = 0.25$, $Q = 1.72$, $s = 2$, $d = 2.1$.

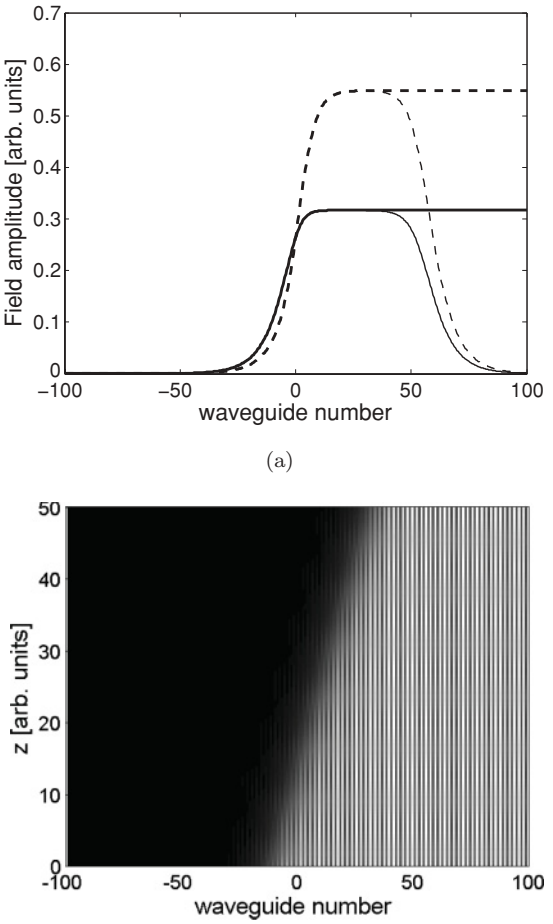

FIG. 6. (a) Example of a flat-top (thin lines) and a kink (thick lines) soliton. Here $\epsilon = 0.25$, $Q = 1.786\,553\,604\,650\,208$ for the dark soliton ($Q = 1.786\,553\,7$ for the flat-top soliton), $s = 2$, $d = 2.5$, $v = 0.5$. (b) Field evolution along the array for the kink soliton.

Hamiltonian: in this case the heteroclinic orbit connecting the two points gives rise to a kink soliton [left inset of Fig. 4(a)]. As Q approaches the existence limit defined by (11), bright solitons become wider and eventually take a kinklike shape. An example of this kind of solution is reported in Fig. 6(a). Figure 6(b) shows the propagation of the kink soliton with velocity $v = 0.5$.

IV. CONCLUSIONS

We have analyzed a model describing light propagation in a binary array, accounting for alternating positive and negative linear coupling as well as nonuniform nonlinearity. This model can be applied in different physical settings such as plasmonic, Bragg, and photonic crystal waveguides. We derived exact bright and kink soliton solutions in the long-wavelength (i.e., continuous) limit. Such solitons display several interesting and unusual features, unique to this type of waveguide structure, and are possible even in the case of alternating focusing-defocusing nonlinearity.

ACKNOWLEDGMENTS

We acknowledge helpful discussions with Professor A. B. Aceves and Professor S. Wabnitz. The work was done in part under the UniBSMIT-MechE faculty exchange program cosponsored by the CARIPLO Foundation, Italy under Grant No. 2008-2290. C.D.A. and M.C. acknowledge financial support from the Air Force Office of Scientific Research, Air Force Material Command, USAF, under Grant No. FA8655-10-1-3083.

[1] F. Lederer, G. I. Stegeman, D. N. Christodoulides, G. Assanto, M. Segev, and Y. Silberberg, Phys. Rep. **463**, 1 (2008).
[2] D. N. Christodoulides and R. I. Joseph, Opt. Lett. **13**, 794 (1988).
[3] A. B. Aceves, C. De Angelis, S. Trillo, and S. Wabnitz, Opt. Lett. **19**, 332 (1994).
[4] A. B. Aceves, C. De Angelis, T. Peschel, R. Muschall, F. Lederer, S. Trillo, and S. Wabnitz, Phys. Rev. E **53**, 1172 (1996).
[5] H. S. Eisenberg, Y. Silberberg, R. Morandotti, A. R. Boyd, and J. S. Aitchison, Phys. Rev. Lett. **81**, 3383 (1998).
[6] A. A. Sukhorukov and Y. S. Kivshar, Phys. Rev. E **65**, 036609 (2002).
[7] A. Szameit, I. L. Garanovich, M. Heinrich, A. A. Sukhorukov, F. Dreisow, T. Pertsch, S. Nolte, A. Tuennermann, and Yu. S. Kivshar, Nature Phys. **5**, 271 (2009).
[8] N. K. Efremidis, S. Sears, D. N. Christodoulides, J. W. Fleischer, and M. Segev, Phys. Rev. E **66**, 046602 (2002).
[9] H. S. Eisenberg and Y. Silberberg, Phys. Rev. Lett. **85**, 1863 (2000).
[10] A. A. Sukhorukov and Y. S. Kivshar, Opt. Lett. **27**, 2112 (2002).
[11] R. Morandotti, D. Mandelik, Y. Silberberg, J. S. Aitchison, M. Sorel, D. N. Christodoulides, A. A. Sukhorukov, and Y. S. Kivshar, Opt. Lett. **29**, 2890 (2004).
[12] A. A. Sukhorukov and Y. S. Kivshar, Opt. Lett. **30**, 1849 (2005).
[13] S. Longhi, Opt. Lett. **31**, 1857 (2006).
[14] M. Guasoni, A. Locatelli, and C. De Angelis, J. Opt. Soc. Am. B **25**, 1515 (2008).
[15] M. Guasoni, M. Conforti, and C. De Angelis, Opt. Commun. **283**, 1161 (2010).
[16] C. M. de Sterke, L. C. Botten, A. A. Asatryan, T. P. White, and R. C. McPhedran, Opt. Lett. **29**, 1384 (2004).
[17] M. Guasoni, M. Conforti, and C. De Angelis, Opt. Lett. **33**, 2362 (2008).
[18] S. H. Nam, E. Ulin-Avila, G. Bartal, and X. Zhang, Opt. Lett. **35**, 1847 (2010).
[19] S. H. Nam, A. J. Taylor, and A. Efimov, Opt. Express **18**, 10120 (2010).
[20] N. K. Efremidis, P. Zhang, Z. Chen, D. N. Christodoulides, C. E. Rüter, and Detlef Kip, Phys. Rev. A **81**, 053817 (2010).
[21] W. Chen and D. L. Mills, Phys. Rev. Lett. **58**, 160 (1987).
[22] D. L. Mills and S. E. Trullinger, Phys. Rev. B **36**, 947 (1987).
[23] A. B. Aceves and S. Wabnitz, Phys. Lett. A **141**, 37 (1989).
[24] C. M. de Sterke, D. G. Salinas, and J. E. Sipe, Phys. Rev. E **54**, 1969 (1996).
[25] C. Conti and S. Trillo, Phys. Rev. E **64**, 036617 (2001).
[26] H. Alatas, A. A. Iskandar, M. O. Tjia, and T. P. Valkering, Phys. Rev. E **73**, 066606 (2006).
[27] H. Alatas, Phys. Rev. A **76**, 023801 (2007).
[28] A. Marini, A. V. Gorbach, and D. V. Skryabin, Opt. Lett. **35**, 3532 (2010).
[29] Y. Liu, G. Bartal, D. A. Genov, and X. Zhang, Phys. Rev. Lett. **99**, 153901 (2007).
[30] N. K. Efremidis and K. Hizanidis, Opt. Express **13**, 10751 (2005).